 doi:10.20944/preprints202102.0583.v1

Article

INVESTIGATIONS ON DYNAMICAL STABILITY IN 3D QUADRUPOLE ION TRAPS

Bogdan M. Mihalcea [1] and Stephen Lynch [2]

[1] Natl. Inst. for Laser, Plasma and Radiation Physics (INFLPR), Atomiştilor Str. Nr. 409, 077125 Măgurele, Romania; bogdan.mihalcea@inflpr.ro
[2] Department of Computing and Mathematics, Manchester Metropolitan University, Manchester M1 5GD, UK; S.Lynch@mmu.ac.uk

Abstract: We firstly discuss classical stability for a dynamical system of two ions levitated in a 3D Radio-Frequency (RF) trap, assimilated with two coupled oscillators. The system dynamics is characterized using a well established model that relies on two control parameters: the axial angular moment and the ratio between the radial and axial trap pseudo-oscillator characteristic frequencies. We augment this model and employ the Hessian matrix of the potential function in an attempt to better describe dynamical stability and the critical points. Our approach is then used to explore quantum stability in case of strongly coupled Coulomb many-body systems and establish a technique aimed at determining the critical points. Finally, we apply the model in case of a 3D Quadrupole Ion Trap (QIT) with axial symmetry, for which we obtain the associated Hamilton function. A different approach is used to better characterize many-body dynamics in combined (Paul and Penning) traps, with applications such as stable trapping of antimatter or fundamental tests of the Standard Model. The ion distribution can be described by means of numerical modeling, based on the Hamilton function we assign to the system. The approach we introduce is effective to infer the parameters of distinct types of traps by applying a cohesive method.

Keywords: radiofrequency trap; dynamical stability; eigenfrequency; Paul and Penning trap; Hessian matrix; Hamilton function; bifurcation diagram.

PACS: 37.10.Ty; 02.30.-f; 02.40.Xx

1. Introduction

The advent of ion traps has led to remarkable progress in modern quantum physics, in atomic and nuclear physics, QED theory, high precision measurements of the magnetic moments of leptons or use of optical transitions in highly charged ions to search for variations of the fine structure constant α [1,2]. Experiments with ion traps also enable ultrahigh resolution spectroscopy experiments, mass spectrometry and quantum metrology measurements of fundamental quantities such as the electron and positron g-factors [1,3]. Ion traps are also employed for quantum engineering [4], searches for dark matter, dark energy, and extra forces [5], Quantum Information Processing (QIP) and quantum metrology [6,7], geodesy [8], investigations of strongly coupled Coulomb systems (SCCS) [9,10] etc.

Scientists can now trap single atoms or photons, acquire excellent control on their quantum states (inner and outer degrees of freedom) and precisely track their evolution by the time [11,12]. A single ion or an ensemble of ions can be secluded with respect to external perturbations, then engineered in a distinct quantum state and trapped in ultrahigh vacuum for long periods of time (months to years) under conditions of dynamical stability. Ion localization results in unique features such as extremely high atomic line quality factors under minimum perturbation by the environment [13]. As

 doi:10.20944/preprints202102.0583.v1

ions are well isolated with respect to the surrounding environment, the superposition states required for quantum computation [14] can live for a relatively long time. The remarkable control accomplished by employing ion traps has led to remarkable progress in quantum engineering [15,16].

Trapping and cooling techniques applied to ions and charged electric particles enable individual addressing and accurate control of quantum states [3,17]. Such investigations allow scientists to perform fundamental tests of quantum mechanics and general relativity, to perform matter and anti-matter tests of the Standard Model, or to perform studies with respect to the spatio-temporal variation of the fundamental constants in physics at the cosmological scale [1,5]. Ion traps are versatile tools used for precision mass measurements or to build optical frequency clocks that will lead to a future redefinition of the SI second [2,18]. Ion traps are also responsible for notable breakthroughs in quantum engineering of space and time [5] and quantum information processing [19]. Moreover, there is a large interest towards quantum many-body physics in trap arrays, with an aim to achieve systems of many interacting spins, represented by qubits in individual microtraps [14–16].

A problem of large interest concerns the strong outcome of the trapped ion dynamics on the achievable resolution of many experiments, and the paper builds exactly in this direction. Fundamental understanding of this problem can be achieved by using analytical and numerical methods which take into account different trap geometries and various cloud sizes. The other issue lies in performing quantum engineering (quantum optics) experiments and high-resolution measurements by developing and implementing different interaction protocols.

Other applications of interest span high-resolution spectroscopy and mass spectrometry [3,20], studies of quantum chaos and integrability [21,22], as well as studies on the multi body dynamics of strongly coupled Coulomb systems (SCCS) [23]. The trapping potential in a RF trap harmonically confines ions in the region where the field exhibits a minimum, under conditions of dynamical stability [3,24]. Hence, a trapped ion can be regarded as a quantum harmonic oscillator [25–28].

1.1. Investigations on classical and quantum dynamics using ion traps

A detailed experimental and theoretical investigation with respect to the dynamics of two-, three-, and four-ion crystals close to the Mathieu instability is presented in [29], where an alytical model is introduced that is later used in a large number of papers to characterize regular and nonlinear dynamics for systems of trapped ions in 3D QIT. We also use this model in our paper and extend it. Numerical evidence of quantum manifestation of order and chaos for ions levitated in a Paul trap is explored in [30], where it is suggested that at the quantum level one can use the quasienergy states statistics to discriminate between integrable and chaotic regimes of motion. Double well dynamics for two trapped ions (in a Paul or Penning trap) is explored in [31], where the RF-drive influence in enhancing or modifying quantum transport in the chaotic separatrix layer is also discussed. Irregular dynamics of a single ion confined in electrodynamic traps that exhibit axial symmetry is explored in [32], by means of analytical and numerical methods. It is also established that period-doubling bifurcations represent the preferred route to chaos.

Ion dynamics of a parametric oscillator in a RF octupole trap is examined in [33,34] with particular emphasis on the trapping stability, which is demonstrated to be position dependent. In Ref. [35] quantum models are introduced to describe multi body dynamics for SCCS stored in a 3D QIT that exhibits axial (cylindrical) symmetry.

A trapped and laser cooled ion that undergoes interaction with a succession of stationary-wave laser pulses may be regarded as the realization of a parametric nonlinear oscillator [36]. Ref. [37] uses numerical methods to explore chaotic dynamics of a particle in a nonlinear 3D QIT trap, which undergoes interaction with a laser field in a quartic potential, in presence of an anharmonic trap potential. The equation of motion is similar

 doi:10.20944/preprints202102.0583.v1

to the one that portrays a forced Duffing oscillator with a periodic kicking term. Fractal attractors are identified for special solutions of ion dynamics. Similarly to Ref. [32], frequency doubling is demonstrated to represent the favourite route to chaos. An experimental confirmation of the validity of the results obtained in [37] can be found in Ref. [38], where stable dynamics of a single trapped and laser cooled ion oscillator in the nonlinear regime is explored.

Charged microparticles stored in a RF trap are characterized either by periodic or irregular dynamics, where in the latter case chaotic orbits occur [39]. Ref. [40] explores dynamical stability for an ion confined in asymmetrical, planar RF ion traps, while establishing that the equations of motion are coupled. Quantum dynamics of ion crystals in RF traps is explored in [41], where stable trapping is discussed along with the validity of the pseudopotential approximation. A phase space study of surface electrode ion traps (SET) that explores integrable, chaotic and combined dynamics is performed in [42], with an emphasis on the integrable and chaotic motion of a single ion. The nonlinear dynamics of an electrically charged particle stored in a RF multipole ion trap is investigated in [43]. An in-depth study of the random dynamics of a single trapped and laser cooled ion that emphasizes nonequilibrium dynamics, is performed in Ref. [17]. Classical dynamics and dynamical quantum states of an ion are investigated in [44], considering the effects of the higher order terms of the trap potential. On the other hand, the method suggested in [45] can be employed to characterize ion dynamics in 2D and 3D QIT traps.

All the studies previously described open new directions of action towards an in-depth exploration of the dynamical equilibrium at the atomic scale, as the subject is extremely actual. In our paper we perform a classical study of the dynamical stability for trapped ion systems (Sec. 2), based on the model introduced in [29,31]. We use the dynamical systems theory to characterize the time evolution of two coupled oscillators in a RF trap, depending on the chosen control parameters. We consider the pseudopotential approximation regime, where the motion is integrable only for discrete values of the ratio between the axial and the radial frequencies of the secular motion. The associated dynamics is shown to be quasiperiodic or ergodic. The Morse theory is then applied to qualitatively analyze system stability. The results are extended to many body strongly coupled trapped ion systems, locally studied in the vicinity of equilibrium configurations that identify ordered structures. These equilibrium configurations exhibit a large interest for quantum computing. Section 4 explores quantum stability and ordered structures for many body dynamics (assuming the ions are identical) in a RF trap. We find the system energy and introduce a method (model) that supplies the elements of the Hessian matrix of the potential function for a critical point. Section 5 applies the model suggested in Section 4. Collective models are introduced and we build integrable Hamiltonians which admit dynamic symmetry groups. We particularize this Hamiltonian function for systems of trapped ions in combined (Paul and Penning) traps with axial symmetry. An improved model results by which multi-particle dynamics in a 3D QIT is associated with dynamic symmetry groups [46–48] and collective variables. The ion distribution in the trap can be described by employing numerical programming, based on the Hamilton function we obtain. This alternative technique can be very helpful to perform a unitary description of the parameters of different types of traps in an integrated approach.

2. Analytical model

2.1. Dynamical stability for two coupled oscillators in a radiofrequency trap

We investigate classical stability for two coupled oscillators (ions) of mass m_1 and m_2, respectively, levitated in a 3D radiofrequency (RF) Quadrupole Ion Trap (QIT). The constants of force are denoted as k_1 and k_2, respectively. Ion dynamics restricted to the $x-y$ plane is described by a set of coupled equations:

Preprints (www.preprints.org) | NOT PEER-REVIEWED | Posted: 25 February 2021 doi:10.20944/preprints202102.0583.v1

$$\begin{cases} m_1\ddot{x} = -k_1 x + b(x-y) \\ m_2\ddot{y} = -k_2 y - b(x-y)\,, \end{cases} \tag{1}$$

where b stands for the parameter that characterizes Coulomb repulsion between ions. The control parameters for the trap are:

$$k_i = \frac{m_i q_i^2 \Omega}{8}\,,\quad q_i = 4\frac{Q_i}{m_i}\frac{V_0}{(z_0\Omega)^2}\,;\; i = 1,2, \tag{2}$$

where we use the pseudopotential approximation with Ω the frequency of the micromotion. Higher order terms in the Mathieu equation [3,49] that portrays ion motion are discarded. V_0 denotes the RF trapping voltage and Q_i represents the electric charge of the ion labeled as i. The Coulomb constant of force is $b \equiv 2Q^2/r^3 < 0$, resulting from a series expansion of Q^2/r^2 about a mean deviation of the ion with respect to the trap centre $r_0 \equiv (x_0 - y_0) < 0$, established by the initial conditions.

The expressions of the kinetic and potential energy are:

$$T = \frac{m_1\dot{x}^2}{2} + \frac{m_2\dot{y}^2}{2}\,,\; U = \frac{k_1 x^2}{2} + \frac{k_2 y^2}{2} + \frac{1}{2}\,b(x-y)^2. \tag{3}$$

It is assumed that the ions share equal electric charges $Q_1 = Q_2$. We denote

$$k_1 = 2Q_1\beta_1\,,\quad \beta_1 = \frac{4Q_1V_0^2}{m_1\Omega^2\xi^4} - \frac{2U_0}{\xi^2}\,, \tag{4}$$

with $\xi^2 = r_0^2 + 2z_0^2$, where r_0 and z_0 denote the trap semiaxes. We assume $U_0 = 0$ (the d.c. trapping voltage) and consider r_0 as negligible. The trap control parameters are U_0, V_0, ξ and k_i. We select an electric potential $V = 1/|z|$ and we perform a series expansion around $z_0 > 0$, with $z - z_0 = x - y$. The potential energy can be then cast into:

$$U = \frac{k_1 x_1^2}{2} + \frac{k_2 x_2^2}{2} + \frac{1}{4\pi\varepsilon_0}\frac{Q_1Q_2}{|x_1 - x_2|}\,, \tag{5}$$

The Hamilton principle states the system is stable if the potential energy U exhibits a minimum

$$k_{1,2}x_{1,2} \mp \lambda = 0\;\;,\;\; \lambda = \frac{1}{4\pi\varepsilon_0}\frac{Q_1Q_2}{|x_1 - x_2|^2}\,. \tag{6}$$

Then

$$k_1x_1 + k_2x_2 = 0\,,\; x_{1\,\min} = \frac{\lambda}{k_1}\,,\; x_{2\,\min} = -\frac{\lambda}{k_2}\,. \tag{7}$$

Equation

$$\lambda = \sqrt[3]{\frac{1}{4\pi\varepsilon_0}\frac{k_1^2k_2^2}{(k_1+k_2)^2}\,Q_1Q_2}\,, \tag{8}$$

supplies the points of minimum, x_1 and x_2, for an equilibrium state. We choose

$$z_0 = x_{1\,\min} - x_{2\,\min} = \lambda\frac{k_1k_2}{k_1+k_2} \tag{9}$$

and denote

$$z = x_1 - x_2\,,\; x_1 = x_{1\,\min} + x\,,\; x_2 = x_{2\,\min} + y\,, \tag{10}$$

with $z = z_0 + x - y$. Eq. (8) gives us

$$\frac{Q_1Q_2}{4\pi\varepsilon_0} = \lambda^3\left(\frac{k_1k_2}{k_1+k_2}\right)^2 = \lambda z_0^2\,. \tag{11}$$

Preprints (www.preprints.org) | NOT PEER-REVIEWED | Posted: 25 February 2021 doi:10.20944/preprints202102.0583.v1

We turn back to eq. (5), then make use of eqs. (7) and (10) to express the potential energy as

$$U = \frac{k_1}{2}\left(x_{1\,\mathrm{min}}^2 + x^2\right) + \frac{k_2}{2}\left(x_{2\,\mathrm{min}}^2 + y^2\right) + \lambda z_0 + \frac{\lambda}{z_0}(z - z_0)^2 - \dots \tag{12}$$

From eq. (3) we obtain $b/2 = \lambda/z_0$. When the potential energy is minimum the system is stable.

2.2. Solutions of coupled system of equations

We seek solutions of the coupled system of equations (1) of the form

$$x = A\sin\omega t\,, \quad y = B\sin\omega t\,. \tag{13}$$

The Wronskian determinant of the resulting system of equations must be zero for a stable system

$$\begin{vmatrix} b - k_1 + m_1\omega^2 & -a \\ -b & b - k_2 + m_2\omega^2 \end{vmatrix} = 0\,. \tag{14}$$

The determinant allows us to construct the characteristic equation:

$$\left(b - k_1 + m_1\omega^2\right)\left(b - k_2 + m_2\omega^2\right) - b^2 = 0 \tag{15}$$

The discriminant of eq. (15) can be cast as

$$\Delta = [m_1(b - k_2) - m_2(b - k_1)]^2 + 4m_1m_2b^2 \tag{16}$$

The system admits solutions if the determinant is zero, as stated above. Hence, a solution of eq. (15) would be:

$$\omega_{1,2}^2 = \frac{m_1(k_2 - b) + m_2(k_1 - b) \pm \sqrt{\Delta}}{2m_1m_2} \tag{17}$$

Then, we find a solution for the system of coupled oscillators

$$x_1 = C_1\sin(\omega_1 t + \varphi_1) + C_2\sin(\omega_2 t + \varphi_2)\,, \tag{18a}$$
$$y_1 = C_3\sin(\omega_1 t + \varphi_3) + C_4\sin(\omega_2 t + \varphi_4)\,, \tag{18b}$$

which describes a superposition of two oscillations characterized by the secular frequencies ω_1 and ω_2, that is to say the system eigenfrequencies. Assuming that $b \ll k_{1,2}$ in eq. (15) the strong coupling condition is

$$\left|\frac{b}{k_i}\right| \gg \left|\frac{m_1 - m_2}{m_2}\right|, \tag{19}$$

where the modes of oscillation are

$$\omega_1^2 = \frac{1}{2}\left(\frac{k_1}{m_1} + \frac{k_2}{m_2}\right). \tag{20}$$

$$\omega_2^2 = \frac{1}{2}\left(\frac{k_1 - 2b}{m_1} + \frac{k_2 - 2b}{m_2}\right). \tag{21}$$

By exploring the phase relations between the solutions of eq. (1), we can ascertain that the ω_1 mode corresponds to a translation of the ions (the distance r_0 between ions does not fluctuate), while the Coulomb repulsion remains steady as b is absent in eq. (20). The axial current produced by this mode of translation can be detected (electronically). In the ω_2 mode the distance between the ions fluctuates about a fixed centre of mass (CM), case when both the electric current and signal are zero. Optical detection is possible in the ω_2 mode, even if electronic detection is not feasible. As a consequence, for collective

Preprints (www.preprints.org) | NOT PEER-REVIEWED | Posted: 25 February 2021 doi:10.20944/preprints202102.0583.v1

modes of motion only a peak of the mass is detected, that corresponds to the ion average mass. In case of weak coupling the inequality in eq. (19) overturns, and from eq. (17) we derive

$$\omega_{1,2}^2 = (k_{1,2} - b)/m_{1,2}\,, \tag{22}$$

which means that each mode of the dynamics matches a single mass, while resonance is shifted with the parameter b. In addition, within the limit of equal ion mass $m_1 = m_2$, the strong coupling requirement in eq. (19) is always fulfilled regardless of how weak is the Coulomb coupling. This renders the weak coupling condition unsuitable in practice.

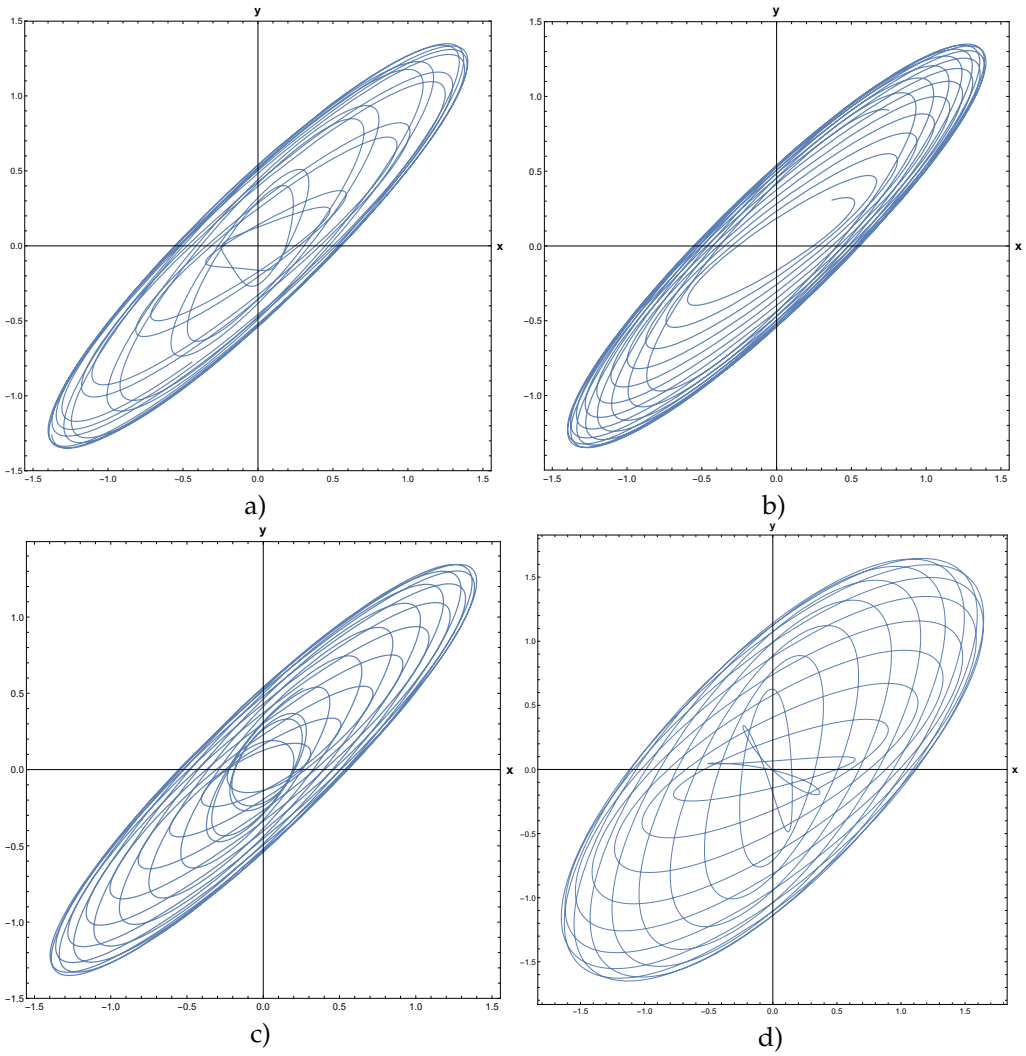

Figure 1. Phase portraits for the coupled oscillators system with initial conditions $C_1 = 0.8, C_2 = 0.6, C_3 = 0.75, C_4 = 0.6, \varphi_1 = \pi/3, \varphi_2 = \pi/4, \varphi_3 = \pi/2, \varphi_4 = \pi/3$: (a) $\omega_1/\omega_2 = 1.71/1.93$. The dynamics is ergodic; (b) $\omega_1/\omega_2 = 1.78/1.96$. quasiperiodic dynamics (c) $\omega_1 = 1.96, \omega_2 = 1.85$; Ion dynamics is ergodic. (d) $C_1 = 0.75, C_2 = 0.9, C_3 = 0.8, C_4 = 0.85, \varphi_1 = \pi/5, \varphi_2 = \pi/6, \varphi_3 = \pi/3, \varphi_4 = \pi/2, \omega_1 = 1.8, \omega_2 = 1.7$. Ion dynamics is quasiperiodic.

Figure 1 (a) illustrates the phase portrait for a system of two coupled oscillators in a RF trap, where the eigenfrequencies ratio is $\omega_1/\omega_2 = 1.71/1.93$. When the eigenfrequencies ratio is a rational number $\omega_1/\omega_2 \in \mathbb{Q}$, the solutions of the equations of motion (18) are periodic trajectories and ion dynamics is regular. In case when the eigenfrequencies ratio is an irrational number $\omega_1/\omega_2 \notin \mathbb{Q}$, iterative rotations occur around a certain point [50] that are called *ergodic*, according to the theorem of Weyl. We have illustrated the solutions 18 of the equations of motions in Figure 1 and Figure 2, to show that ion dynamics is generally quasiperiodic and stable. There are also a few cases

Preprints (www.preprints.org) | NOT PEER-REVIEWED | Posted: 25 February 2021 doi:10.20944/preprints202102.0583.v1

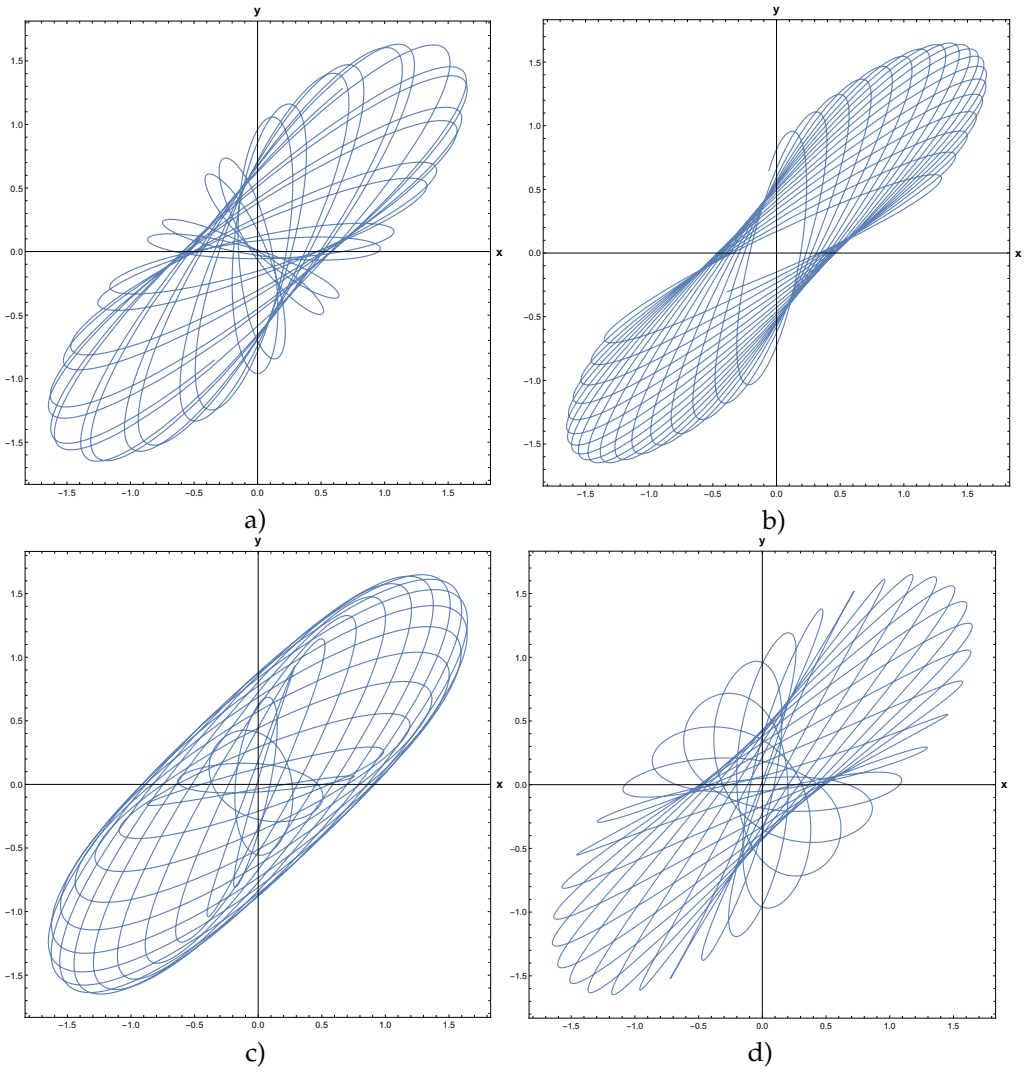

Figure 2. Phase portrait for the coupled oscillators system with initial conditions $C_1 = 0.75, C_2 = 0.9, C_3 = 0.8, C_4 = 0.85$: (a) $\varphi_1 = \pi/4, \varphi_2 = \pi/2, \varphi_3 = \pi/3, \varphi_4 = \pi/5, \omega_1/\omega_2 = 1.76/1.95$ ergodic motion; (b) case $\varphi_1 = \pi/4, \varphi_2 = \pi/2, \varphi_3 = \pi/3, \varphi_4 = \pi/4, \omega_1 = 1.81, \omega_2 = 1.88$, the associated dynamics is clearly quasiperiodic ; (c) $\varphi_1 = \pi/6, \varphi_2 = \pi/5, \varphi_3 = \pi/2, \varphi_4 = \pi/4, \omega_1 = 1.8, \omega_2 = 1.9$. Ion dynamics is quasiperiodic; (d) $\varphi_1 = \pi/6, \varphi_2 = \pi/4, \varphi_3 = \pi/2, \varphi_4 = \pi/8, \omega_1 = 1.5, \omega_2 = 1.9$, the system exhibits quasiperiodic dynamics.

which illustrate ergodic dynamics [50] and the occurrence of what may be interpreted as iterative rotations. According to Figures 1 and 2, by extending the motion in 3D we can ascertain that the trajectory executes quasiperiodic motion on the surface of a torus, referred to as a Kolmogorov-Arnold-Moser (KAM) torus [51]. By choosing various initial conditions different KAM tori can be generated.

We have integrated the equations of motion 1 to explore ion dynamics and illustrate the associated power spectra [52], as shown in Figure 3 and Figure 4. The numerical simulations performed clearly demonstrate that ion dynamics is dominantly quasiperiodic.

A recent paper, Ref. [53], describes an electrodynamic ion trap in which the electric quadrupole field oscillates at two different frequencies. The authors report simultaneous tight confinement of ions with extremely different charge-to-mass ratios, e.g. singly ionized atomic ions together with multiply charged nanoparticles. The system represents the equivalent of two *superimposed* RF traps, where each one of them operates close to a frequency optimized in order to achieve tight storage for one of the species involved, which leads to strong and stable confinement for both particle species used.

Preprints (www.preprints.org) | NOT PEER-REVIEWED | Posted: 25 February 2021 doi:10.20944/preprints202102.0583.v1

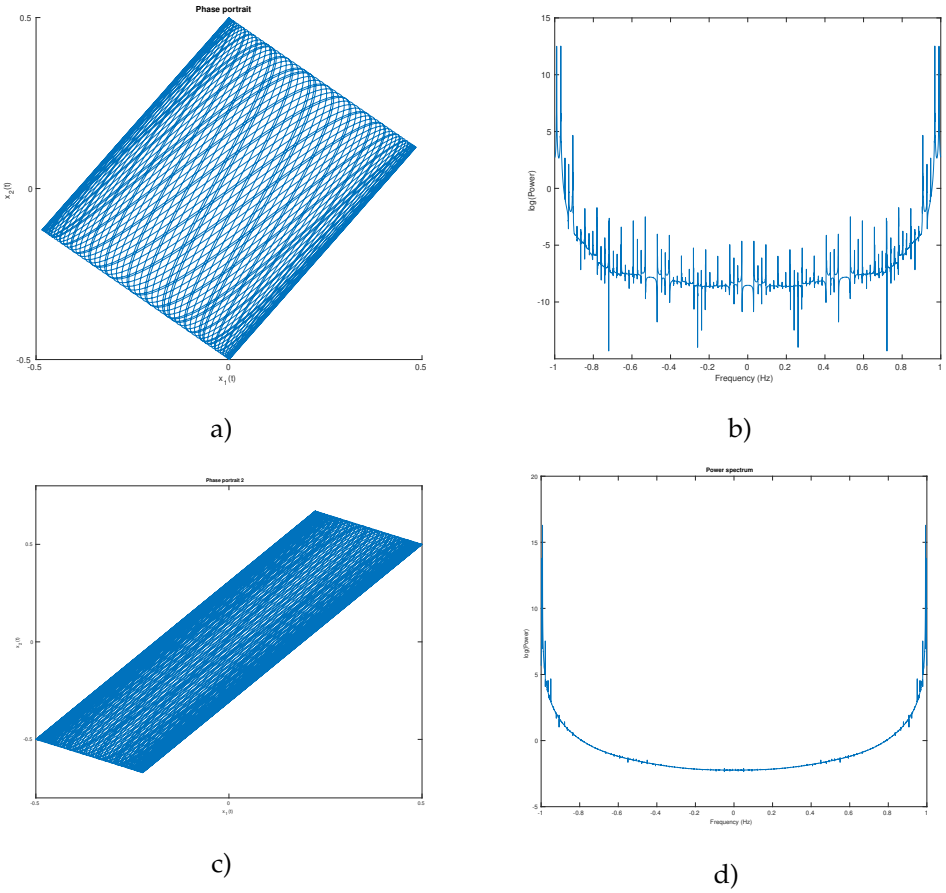

Figure 3. Phase portraits and power spectra for the two coupled oscillator system obtained by integrating the equations of motion 1: case (a) initial conditions $\dot{x}(0) = 0, \dot{y}(0) = 0.5, x(0) = 0, y(0) = 0$, parameter values: $b = 2, k_1 = 4, k_2 = 5, m_1 = 1, m_2 = 1$. Ion dynamics is quasiperiodic, as illustrated by the associated power spectra (b). We denote $x = x(1)$ and $y = x(2)$; case (c) initial conditions $\dot{x}(0) = 0.5, \dot{y}(0) = 0.5, x(0) = 0, y(0) = 0$, parameter values: $b = 1, k_1 = 2, k_2 = 3, m_1 = 1, m_2 = 1$.

3. Dynamic stability for two oscillators levitated in a RF trap

3.1. System Hamiltonian. Hessian matrix approach

If we consider two ions with equal electric charges, their relative motion is described by the equation [29,31,32]

$$\frac{d^2}{dt^2}\begin{bmatrix} x \\ y \\ z \end{bmatrix} + [a + 2q\cos(2t)]\begin{bmatrix} x \\ y \\ -2z \end{bmatrix} = \frac{\mu_x^2}{|\mathbf{r}|^3}\begin{bmatrix} x \\ y \\ z \end{bmatrix}, \tag{23}$$

where $\vec{r} = x_1 - x_2$, $\mu_x = \sqrt{a + \frac{1}{2}q^2}$ represents the dimensionless radial secular (pseudo-oscillator) characteristic frequency [54], while a and q stand for the adimensional trap parameters in the Mathieu equation, namely

$$a = \frac{8QU_0}{m\Omega^2(r_0^2 + 2z_0^2)}, \quad q = \frac{4QV_0}{m\Omega^2(r_0^2 + 2z_0^2)}.$$

U_0 and V_0 denote the d.c and RF trap voltage, respectively, Q stands for the electric charge of the ion, Ω represents the RF drive frequency, while r_0 and z_0 are the trap radial and axial dimensions. For $a, q \ll 1$ the pseudopotential approximation is valid. In such

Preprints (www.preprints.org) | NOT PEER-REVIEWED | Posted: 25 February 2021 doi:10.20944/preprints202102.0583.v1

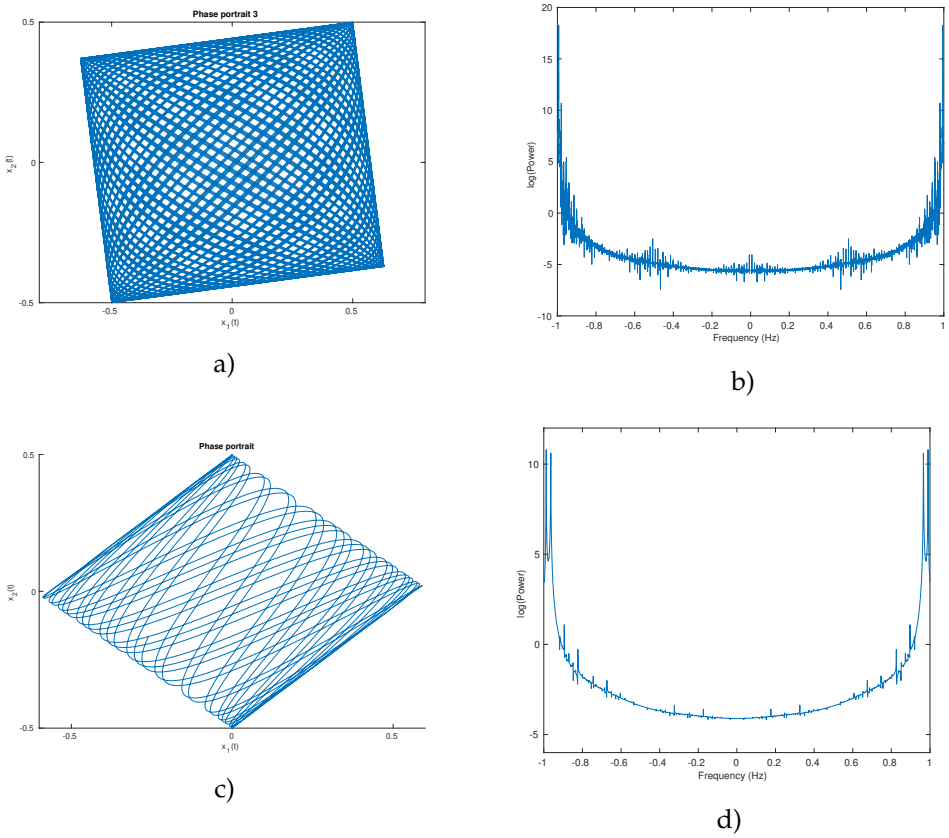

Figure 4. Phase portraits and power spectra for the two ion system obtained by integrating the equations of motion 1: case (a) initial conditions $\dot{x}(0) = 0.5, \dot{y}(0) = 0.5, x(0) = 0, y(0) = 0$, parameter values: $b = 3, k_1 = 99, k_2 = 102, m_1 = 10, m_2 = 13$. Ion dynamics is quasiperiodic, as illustrated by the associated power spectra (b); case (c) initial conditions $\dot{x}(0) = 0, \dot{y}(0) = 0.5, x(0) = 0, y(0) = 0$, parameter values: $b = 2, k_1 = 4, k_2 = 5, m_1 = 5, m_2 = 7$

case we can associate an autonomous Hamilton function to the system described by eq. (23), which we express in scaled cylindrical coordinates (ρ, ϕ, z) as [29]

$$H = \frac{1}{2}\left(p_\rho^2 + p_z^2\right) + U(\rho, z)\,, \tag{24}$$

where

$$U(\rho, z) = \frac{1}{2}\left(\rho^2 + \lambda^2 z^2\right) + \frac{\nu^2}{2\rho^2} + \frac{1}{r}\,, \tag{25}$$

with $r = \sqrt{\rho^2 + z^2}$, $\lambda = \mu_z/\mu_x$, and $\mu_z = \sqrt{2(q^2 - a)}$. ν denotes the scaled axial (z) component of the angular momentum L_z and it is a constant of motion, while μ_z represents the second secular frequency [29]. We emphasize that both λ and ν are strictly positive control parameters. For arbitrary values of ν and for positive discrete values of $\lambda = 1/2, 1, 2$, eq. (25) is integrable and even separable, excluding the case when $\lambda = 1/2$ and $|\nu| > 0$ ($\nu \neq 0$), as stated in [30].

The equations of the relative motion corresponding to the Hamiltonian function described by eq. (24) can be cast into [29,30]:

$$\ddot{z} = \frac{z}{r^{3/2}} - \lambda^2 z\,, \tag{26a}$$

$$\ddot{\rho} = \frac{\rho}{r^{3/2}} - \rho + \frac{\nu^2}{\rho^3}\,, \tag{26b}$$

Preprints (www.preprints.org) | NOT PEER-REVIEWED | Posted: 25 February 2021 doi:10.20944/preprints202102.0583.v1

with $p_\rho = \dot{\rho}$ and $p_z = \dot{z}$. The critical points of the U potential are determined as solutions of the system of equations:

$$\frac{\partial U}{\partial \rho} = \rho - \frac{\nu^2}{\rho^3} - \frac{1}{r^2}\frac{\rho}{r} = 0\,, \tag{27a}$$

$$\frac{\partial U}{\partial z} = \lambda^2 z - \frac{1}{r^2}\frac{z}{r} = 0, \tag{27b}$$

where $\partial r/\partial \rho = \rho/r$ and $\partial r/\partial z = z/r$.

3.2. Solutions of the equations of motion for the two oscillator system

We discuss the solutions of eq. 27, namely

$$z\left(\lambda^2 - \frac{1}{r^3}\right) = 0\,, \tag{28}$$

which leads to a number of two possible cases:
Case 1. $z = 0$. The first equation of the system (27) can be rewritten as

$$\rho - \frac{\nu^2}{\rho^3} - \frac{\rho}{r^3} = 0$$

which gives us $\rho = r$ for $z = 0$. In such case, a function results

$$f(\rho) = \rho^4 - \rho - \nu^2\,,\ f'(\rho) = 4\rho^3 - 1 \tag{29}$$

The second relationship in eq. (29) shows that $\rho = \sqrt[3]{\frac{1}{4}}$ is a point of minimum for $f(\rho)$. In case when $\rho_0 > 0$, for $\nu \neq 0$ and $z_0 = 0$:

$$f(\rho) = \rho_0^4 - \rho_0 - \nu^2 = 0\,.$$

In case when $\nu = 0$ we obtain $f(\rho) = \rho\left(\rho^3 - 1\right) = 0$. Then, the solutions are $\rho_1 = 0$ and $\rho_2 = 1$, where only $\rho_2 = 1$ is a valid solution. Moreover, for $\nu = 0$ and $z_0 = 0$, $\rho_0 = 1$ is a solution.
Case 2. $r^3 = 1/\lambda^2 \Rightarrow$

$$r = \lambda^{-2/3}\,. \tag{30}$$

We return to the system of eqs. (27) and infer

$$\rho = \frac{\sqrt{|\nu|}}{\sqrt[4]{1-\lambda^2}}\,, \tag{31}$$

for $\lambda < 1$. In case when $\lambda \leq 1$ and $\nu \neq 0$, the system admits no solutions. In the scenario when $\lambda < 1, \nu = 0$ we find $\rho = 0$, while in case when $\lambda = 1,\ \nu = 0$ it results that any $\rho \geq 0$ represents a solution. As $r = \sqrt{z^2 + \rho^2}$

$$z = \pm\sqrt{r^2 - \rho^2} = \pm\sqrt{\lambda^{-4/3} - \rho^2} \tag{32}$$

We differentiate among three possible sub-cases
Subcase (i): $\lambda < 1\,, \nu \neq 0$ and

$$z_{12} = \pm\sqrt{\lambda^{-4/3} - \frac{|\nu|}{\sqrt{1-\lambda^2}}}$$

provided that $1 - \lambda^2 > \nu^2\lambda^{8/3}$ or

$$z = 0 \text{ for } 1 - \lambda_c^2 = \nu^2\lambda_c^{8/3}$$

Preprints (www.preprints.org) | NOT PEER-REVIEWED | Posted: 25 February 2021 doi:10.20944/preprints202102.0583.v1

where the c index of λ refers to critical.
Subcase (ii): $\lambda < 1, \nu = 0$ which leads to $\rho = 0$ and $z_{12} = \pm\lambda^{-2/3}$.
Subcase (iii): $\lambda = 1, \nu = 0$ which results in $z_{12} = \pm\sqrt{\lambda^{-4/3} - \rho^2}$, with $\rho \geq 0$.

These are the solutions we find for the equations of motion corresponding to the two coupled oscilators system. After doing the math, the Hessian matrix of the potential U appears as

$$\mathsf{H} = \begin{vmatrix} 1 + \frac{3\nu^2}{\rho^4} - \frac{1}{r^3} + \frac{3\rho^2}{r^5} & \frac{3\rho z}{r^5} \\ \frac{3\rho z}{r^5} & \lambda^2 - \frac{1}{r^3} + \frac{3z^2}{r^5} \end{vmatrix} . \tag{33}$$

The determinant and the trace of the Hessian matrix result as

$$\det \mathsf{H} = \frac{3\nu^2}{\rho^4}\left(\lambda^2 - \frac{1}{r^3} + \frac{3z^2}{r^5}\right) + \lambda^2\left(1 - \frac{1}{r^3} + \frac{3\rho^2}{r^5}\right) - \frac{1}{r^3}\left(1 + \frac{2}{r^3} - \frac{3z^2}{r^2}\right) , \tag{34a}$$

$$\mathrm{Tr}\, \mathsf{H} = 1 + \lambda^2 + \frac{3\nu^2}{\rho^4} + \frac{1}{r^3} . \tag{34b}$$

From eqs. (34) we infer that $\mathrm{Tr}\, \mathsf{H} = 0$. Thus, the Hessian matrix H has at least a strictly positive eigenvalue.

3.3. Critical points. Discussion.

We use eqs. 34 with an aim to investigate the critical points for the system of interest. We consider two distinct cases:
Case 1. $z = 0$ and $r = \rho$. Then eqs. (34) modify appropriately

$$\det \mathsf{H} = \frac{3\nu^2}{\rho^4}\left(\lambda^2 - \frac{1}{\rho^3}\right) + \lambda^2\left(1 + \frac{2}{\rho^3}\right) - \frac{1}{\rho^3}\left(1 + \frac{2}{\rho^3}\right) , \tag{35a}$$

$$\mathrm{Tr}\, \mathsf{H} = 1 + \lambda^2 + \frac{3\nu^2}{\rho^4} + \frac{1}{\rho^3} . \tag{35b}$$

We discriminate among the following sub-cases:
Subcase (i): $\nu = 0,\ z = 0,\ \rho = 1$.
We obtain a system of equations as follows

$$\mathrm{Tr}\, \mathsf{H} = 2 + \lambda^2 > 0 , \tag{36a}$$

$$\det \mathsf{H} = 3\left(\lambda^2 - 1\right) . \tag{36b}$$

Moreover, a tabel results that describes the eigenvalues λ_1 and λ_2 of the Hessian matrix:

	λ_1	λ_2	Critical point
$0 < \lambda < 1$	> 0	> 0	Minimum
$\lambda = 1$	> 0	0	Degeneracy
$\lambda > 1$	> 0	< 0	Saddle point

Only if $\lambda = 1$ the critical point is degenerate. When the determinant of the Hessian matrix of the potential $\det \mathsf{H} \neq 0$ the system is non-degenerate. The system is degenerate if $\det \mathsf{H} = 0$.
Subcase (ii): $z = 0,\ \nu \neq 0$.

The derivatives of a smooth function must be continuous. We now turn back to eq. (29). Then $\nu^2 = \rho\left(\rho^3 - 1\right)$ and

$$\det \mathsf{H} = \left(4 - \frac{1}{\rho^3}\right)\left(\lambda^2 - \frac{1}{\rho^3}\right) . \tag{37}$$

Preprints (www.preprints.org) | NOT PEER-REVIEWED | Posted: 25 February 2021 doi:10.20944/preprints202102.0583.v1

We seek for degenerate critical points (characterized by $\det \mathsf{H} = 0$). We infer $\rho = \lambda^{-2/3}$ or $\rho = 4^{-3}$, which involves two distinct sub-subcases:

a) $\rho = \lambda^{-2/3}$. We return to eq. (27) and infer

$$\lambda^{-8/3} - \lambda^{-2/3} - \nu^2 = 0\,.$$

b) $\rho^4 \geq \rho\,,\ \rho \geq 1$. In such a situation we encounter a point of minimum when $\rho > \lambda^{-2/3}$, while the case $\rho < \lambda^{-2/3}$ implies a saddle point.

Case 2. $r = \lambda^{-4/3}\,,\ z^2 = \lambda^{-4/3} - \rho^2\,.$

In this particular situation, after doing the math eqs. (34) can be recast into

$$\det \mathsf{H} = 12\lambda^2\left(1-\lambda^2\right)\left(1-\lambda^{4/3}\rho^2\right)\ , \tag{38a}$$

$$\mathrm{Tr}\,\mathsf{H} = 4 - \lambda^2 > 0\,, \tag{38b}$$

with $0 \leq \lambda^2 \leq 1$. We differentiate among several sub-cases as follows:

Subcase (i): $\nu = 0\,,\ \lambda^2 = 1$. We further infer $z = \pm\sqrt{\lambda^{-4/3} - \rho^2}$, with $\rho^2 \in \left[-\lambda^{2/3}, \lambda^{2/3}\right]$, $\rho \leq -\lambda^{-8/3}$. Then $\mathrm{Tr}\,\mathsf{H} = 3$ and $\det \mathsf{H} = 0$, which characterizes a generate critical point.

Subcase (ii): $\nu \neq 0\,,\ \lambda^2 = 0$. We are in the case of a degenerate critical point, with $\rho = \sqrt{|\nu|}$. In this particular case $\det \mathsf{H} = 0$ and

$$\nu^2 = \lambda^{-8/3} - \lambda^{-2/3}$$

Subcase (iii): $0 \leq \lambda^2 < 1\,,\ \nu \neq 0$. The critical point is a point of minimum, as $\det \mathsf{H} > 0$:

$$\rho_0 = \frac{\sqrt{|\nu|}}{\sqrt[4]{1-\lambda^2}}\,,\ 1 - \lambda^2 > \nu^2\lambda^{4/3}\,,$$

$$z_{1,2} = \sqrt{\lambda^{-4/3} - \frac{\nu}{\sqrt{1-\lambda^2}}}\,.$$

Subcase (iv): $0 < \lambda^2 < 1\,, \nu = 0$. Then $\rho = 0$ and $\det \mathsf{H} = 0$, which indicates a point of minimum characterized by $z_{12} = \pm\lambda^{-2/3}$.

Subcase (v): Case $\nu = 0\,, \lambda = 0$. In such case we infer $\rho = 0\,, z = 0$. We are in the case of a degenerate critical point as $(\det \mathsf{H} = 0)$.

Subcase (vi): Case $\rho = \lambda^{-2/3}$, $\lambda = \lambda_c$.

$$1 - \lambda_c^2 = \nu^2\lambda_c^{8/3} \tag{39}$$

The critical point is degenerate, with $z = 0$ and $(\det \mathsf{H} = 0)$.

A critical point for which the Hessian matrix is non-singular, is called a non-degenerate critical point. A Morse function admits only non-degenerate critical points that are stable [55]. The degenerate critical points (defined by $\det \mathsf{H} = 0$) compose the bifurcation set, whose image in the control parameter space (more precisely the $\nu - \lambda$ plan) establishes the catastrophe set of equations which defines the separatrix:

$$\nu = \sqrt{\lambda^{-8/3} - \lambda^{-2/3}} \ \text{ or } \ \lambda = 0 \tag{40}$$

To resume, we use the Hessian matrix to better characterize dynamical stability and the critical points of the system. Figure 5 displays the bifurcation diagram for two coupled oscillators confined in a Paul trap. The ion relative motion is characterized by the Hamilton function described by eqs. (24) and (25). The diagram illustrates both stability and instability regions where ion dynamics is integrable and non-integrable, respectively. Ion dynamics is integrable and even separable when $\lambda = 0.5$, $\lambda = 1$, $\lambda = 2$ [30–32].

Preprints (www.preprints.org) | NOT PEER-REVIEWED | Posted: 25 February 2021 doi:10.20944/preprints202102.0583.v1

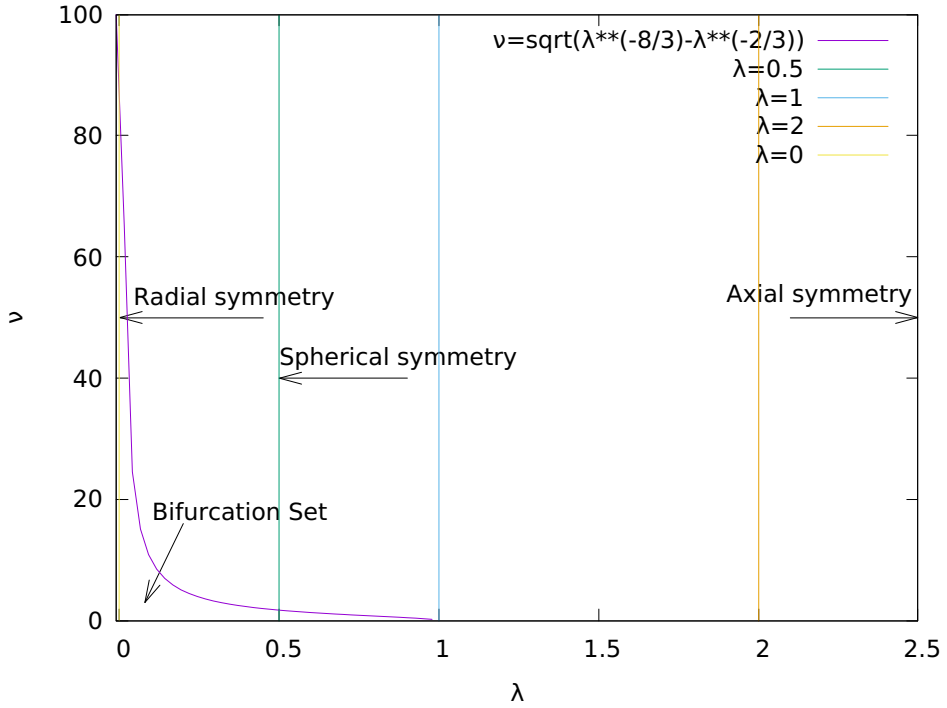

Figure 5. The bifurcation set for a system of two ions confined in a Paul trap.

4. Quantum stability and ordered structures

We investigate a system consisting of N identical ions of mass m_α and electric charge Q_α $(\alpha = 1, 2, \ldots, N)$, confined in a 3D RF (Paul) trap. The coordinate vector of the particle labeled as α is denoted by $\vec{r}_\alpha = (x_\alpha, y_\alpha, z_\alpha)$. A number of $3N$ generalized quantum coordinates $q_{\alpha i}, i = 1, 2, 3$ are associated to the $3N$ degrees of liberty. We also denote $q_{\alpha 1} = x_\alpha$, $q_{\alpha 2} = y_\alpha$, and $q_{\alpha 3} = z_\alpha$. Hence, the kinetic energy for a number of α particles confined in the trap can be expressed as

$$T = \sum_{\alpha=1}^{N} \sum_{i=1}^{3} \frac{1}{2m_\alpha} \dot{q}_{\alpha i}^2 \,, \tag{41}$$

while the potential energy is

$$U = \frac{1}{2} \sum_{\alpha=1}^{N} \sum_{i=1}^{3} k_i q_{\alpha i}^2 + \sum_{1 \le \alpha < \beta \le N} \frac{Q_\alpha Q_\beta}{4\pi\varepsilon_0 |\vec{r}_\alpha - \vec{r}_\beta|} \,, \tag{42}$$

where ε_0 stands for the vacuum permittivity. For a spherical 3D trap: $k_1 = k_2 = k_3$. In case of Paul or Penning 3D QIT $k_1 = k_2$, while the linear 2D Paul trap (LIT) corresponds to $k_3 = 0$, $k_1 = -k_2$. The k_i constants in case of a Paul trap result from the pseudo-potential approximation. The critical points of the system result as:

$$\sum_{\alpha=1}^{N} \Delta_\alpha U = 0 \,, \; \Delta_\alpha = \frac{\partial^2}{\partial x_\alpha^2} + \frac{\partial^2}{\partial y_\alpha^2} + \frac{\partial^2}{\partial z_\alpha^2} \tag{43}$$

$$\Delta U = 0 \text{ or } \frac{\partial U}{\partial q_{\gamma j}} = 0, \;\; \gamma = 1, \ldots, N; \; j = 1, 2, 3. \tag{44}$$

We denote

$$\frac{\partial q_{\alpha i}}{\partial q_{\gamma j}} = \delta_{\alpha\gamma}\delta_{ij} \,, \tag{45}$$

Preprints (www.preprints.org) | NOT PEER-REVIEWED | Posted: 25 February 2021 doi:10.20944/preprints202102.0583.v1

where δ stands for the Kronecker delta function. After doing the math we can write eq. (44) as

$$\frac{\partial U}{\partial q_{\gamma j}} = \frac{1}{2}\sum_{\alpha=1}^{N}\sum_{i=1}^{3} 2k_i q_{\alpha i}\delta_{\alpha\gamma}\delta_{ij} - \sum_{1\leq\alpha<\beta\leq N}\frac{1}{4\pi\varepsilon_0}\frac{Q_\alpha Q_\beta}{|\vec{r}_\alpha - \vec{r}_\beta|^3}\left(q_{\alpha j} - q_{\beta j}\right)\left(\delta_{\alpha\gamma} - \delta_{\beta\gamma}\right), \quad (46)$$

where the second term in eq. (46) represents the energy of the system, and introduce

$$\xi_{\alpha\beta} = \frac{1}{4\pi\varepsilon_0}\frac{Q_\alpha Q_\beta}{|\vec{r}_\alpha - \vec{r}_\beta|^3}, \ \ \alpha \neq \beta. \quad (47)$$

Moreover, $\xi_{\alpha\beta} = \xi_{\beta\alpha}$. After some calculus the system energy can be cast as

$$E = q_{\gamma j}\sum_{\alpha=1}^{N}\xi_{\alpha\gamma} - \sum_{\alpha=1}^{N}\xi_{\alpha\gamma}q_{\alpha j}\,. \quad (48)$$

We use eq. (48) and eq. (46), while the critical points (in particular, the minimums) result as a solution of the system of equations

$$\frac{\partial U}{\partial q_{\gamma j}} = \left(k_j - \sum_{\alpha=1}^{N}\xi_{\alpha\gamma}\right)q_{\gamma j} + \sum_{\alpha=1}^{N}\xi_{\alpha\gamma}q_{\alpha j} = 0, \ \ 1\leq j\leq 3, \ \ 1\leq\alpha\leq N\,. \quad (49)$$

We consider $\bar{q}_{\alpha j}$ to be a solution of the system of equations (49) and obtain

$$U(q) = U(\bar{q}) + \sum_{\alpha=1}^{N}\sum_{j=1}^{3}\frac{\partial U}{\partial q_{\alpha j}}\left(q_{\alpha j} - \bar{q}_{\alpha j}\right) + \frac{1}{2}\sum_{\alpha,\alpha'=1}^{N}\sum_{j,j'=1}^{3}\frac{\partial^2 U}{\partial q_{\alpha j}\partial q_{\alpha' j'}}\left(q_{\alpha j} - \bar{q}_{\alpha j}\right)\left(q_{\alpha' j'} - \bar{q}_{\alpha' j'}\right) + \ldots \quad (50)$$

We further infer

$$\frac{\partial^2 U}{\partial q_{\gamma j}\partial q_{\gamma' j'}} = k_j\delta_{\gamma\gamma'}\delta_{jj'} - \sum_{\alpha=1}^{N}\xi_{\alpha\gamma}\delta_{\gamma\gamma'}\delta_{jj'} - q_{\gamma j}\sum_{\alpha=1}^{N}\frac{\partial\xi_{\alpha\gamma}}{\partial q_{\gamma' j'}} + \sum_{\alpha=1}^{N}\xi_{\gamma\gamma'}\delta_{jj'} + \sum_{\alpha=1}^{N}\frac{\partial\xi_{\alpha\gamma}}{\partial q_{\gamma' j'}}q_{\alpha j}\,. \quad (51)$$

After performing the math (details are supplied in Sec. B) we cast eq. (51) into

$$\frac{\partial^2 U}{\partial q_{\gamma j}\partial q_{\gamma' j'}} = -\left(\sum_{\alpha=1}^{N}\xi_{\alpha\gamma}\right)\delta_{\gamma\gamma'}\delta_{jj'} + \xi_{\gamma\gamma'}\delta_{jj'} + k_j\delta_{\gamma\gamma'}\delta_{jj'} + q_{\gamma j}\sum_{\alpha=1}^{N}\eta_{\alpha\gamma}\left(q_{\alpha j'} - q_{\gamma j'}\right)\left(\delta_{\alpha\gamma'} - \delta_{\gamma\gamma'}\right) - \sum_{\alpha=1}^{N}\eta_{\alpha\gamma}\left(q_{\alpha j'} - q_{\gamma j'}\right)\left(\delta_{\alpha\gamma'} - \delta_{\gamma\gamma'}\right)q_{\alpha j} \quad (52)$$

We search for a fixed solution $q^0_{\gamma j}$ of the system of equations (49). Then, the elements of the Hessian matrix of the potential function U in a critical point of coordinates $q^0_{\gamma j}$ are:

Preprints (www.preprints.org) | NOT PEER-REVIEWED | Posted: 25 February 2021 doi:10.20944/preprints202102.0583.v1

$$\frac{\partial^2 U}{\partial q^0_{\gamma j}\partial q^0_{\gamma' j'}} = k_j\delta_{\gamma\gamma'}\delta_{jj'} + \xi_{\gamma\gamma'}\delta_{jj'} - \left(\sum_{\alpha=1}^{N}\xi_{\alpha\gamma}\right)\delta_{\gamma\gamma'}\delta_{jj'} + \eta_{\gamma\gamma'}\left(q^0_{\gamma j}q^0_{\gamma' j'} - q^0_{\gamma j}q^0_{\gamma j'} - q^0_{\gamma' j}q^0_{\gamma' j'} + q^0_{\gamma' j}q^0_{\gamma j'}\right) + q^0_{\gamma j}q^0_{\gamma j'}\sum_{\alpha=1}^{N}\eta_{\alpha\gamma}\delta_{\gamma\gamma'} + \delta_{\gamma\gamma'}\sum_{\alpha=1}^{N}\eta_{\alpha\gamma}q^0_{\alpha j}q^0_{\alpha j'} - \delta_{\gamma\gamma'}q^0_{\gamma j}\sum_{\alpha=1}^{N}\eta_{\alpha\gamma}q^0_{\alpha j'} - \delta_{\gamma\gamma'}q^0_{\gamma j'}\sum_{\alpha=1}^{N}\eta_{\alpha\gamma}q^0_{\alpha j}\,. \quad (53)$$

5. Hamiltonians for systems of N ions

Collective dynamics for many body systems confined in a 3D QIT that exhibits cylindrical (axial) symmetry is characterized in Refs. [3,35]. We explore a system consisting of N ions in a space with d dimensions, labeled as $\mathbb{R}^d$. The coordinates in the manifold of configurations $\mathbb{R}^d$ are denoted by $x_{\alpha j}$, $\alpha = 1,\ldots,N$, $j = 1,\ldots,d$. In case of linear, planar or 3D (space) models, the number of corresponding dimensions is $d = 1$, $d = 2$ or $d = 3$, respectively. We will further introduce the kinetic energy T, the linear potential energy U_1, the 3D QIT potential energy U and the anharmonic trap potential V:

$$T = \sum_{\alpha=1}^{N}\sum_{j=1}^{d}\frac{1}{2m_\alpha}\,p^2_{\alpha j}\,,\quad U_1 = \frac{1}{2}\sum_{\alpha=1}^{N}\sum_{j=1}^{d}\delta_j x_{\alpha j}\,, \quad (54a)$$

$$U = \frac{1}{2}\sum_{\alpha=1}^{N}\sum_{i,j=1}^{d}\kappa_{ij}x^2_{\alpha j}\,,\quad V = \sum_{\alpha=1}^{N}v(\mathbf{x}_\alpha,t) \quad (54b)$$

where m_α is the mass of an ion labeled by α, $\mathbf{x}_\alpha = (x_{\alpha 1},\ldots,x_{\alpha d})$, while δ_j and κ_{ij} represent functions that ultimately depend on time. The Hamilton function associated to the strongly coupled Coulomb system (SCCS) under investigation is

$$H = T + U_1 + U + V + W\,,$$

where W denotes the interaction potential between the ions.

Under the assumption of equal ion masses we introduce d coordinates x_j of the center of mass (CM)

$$x_j = \frac{1}{N}\sum_{\alpha=1}^{N}x_{\alpha j}\,, \quad (55)$$

and $d(N-1)$ coordinates $y_{\alpha j}$ to account for the relative ion motion

$$y_{\alpha j} = x_{\alpha j} - x_j\,,\quad \sum_{\alpha=1}^{N}y_{\alpha j} = 0\,. \quad (56)$$

We also introduce d collective coordinates s_j and the collective coordinate s, identified as

$$s_j = \sum_{\alpha=1}^{N}y^2_{\alpha j}\,,\ s = \sum_{\alpha=1}^{N}\sum_{j=1}^{d}y^2_{\alpha j}\,. \quad (57)$$

Then

$$\sum_{\alpha=1}^{N}x^2_{\alpha j} = Nx^2_j + \sum_{\alpha=1}^{N}y^2_{\alpha j}\,. \quad (58)$$

$$s_j = \frac{1}{2N}\sum_{\alpha,\beta=1}^{N}\left(x_{\alpha j} - x_{\beta j}\right)^2\,,\quad s = \frac{1}{2N}\sum_{\alpha,\beta=1}^{N}\sum_{j=1}^{d}\left(x_{\alpha j} - x_{\beta j}\right)^2\,. \quad (59)$$

Preprints (www.preprints.org) | NOT PEER-REVIEWED | Posted: 25 February 2021 doi:10.20944/preprints202102.0583.v1

Eq. (59) shows s to symbolize the squared distance measured between the origin (fixed in the CM) and the point that designates the system of N ions in the manifold of configurations. The relation $s = s_0$, with $s_0 > 0$ constant, establishes a sphere of radius $\sqrt{s_0}$ whose centre is located in the origin (of the configurations manifold). When investigating ordered structures of N ions, the trajectory is restricted within a neighbourhood $\|s - s_0\| < \varepsilon$ of this sphere, with ε sufficiently small. At the same time, the collective variable s can be also regarded as a dispersion:

$$s = \sum_{\alpha=1}^{N} \sum_{j=1}^{d} \left(x_{\alpha j}^2 - x_j^2 \right) . \tag{60}$$

We now submit $p_{\alpha j}$ moments associated to the coordinates $x_{\alpha j}$. We also introduce d moments p_j of the center of mass (CM) and $d(N-1)$ moments $\xi_{\alpha j}$ of the relative ion motion defined as

$$p_j = \frac{1}{N} \sum_{\alpha=1}^{N} p_{\alpha j} , \;\; \xi_{\alpha j} = p_{\alpha j} - p_j , \;\; \sum_{\alpha=1}^{N} \xi_{\alpha j} = 0 , \tag{61}$$

with $p_{\alpha j} = -i\hbar \left(\partial / \partial x_{\alpha j} \right)$. We denote

$$D_j = \frac{1}{N} \sum_{\alpha=1}^{N} \frac{\partial}{\partial x_{\alpha j}} , \;\; D_{\alpha j} = \frac{\partial}{\partial x_{\alpha j}} - D_j , \;\; \sum_{\alpha=1}^{N} D_{\alpha j} = 0 . \tag{62}$$

In addition

$$\sum_{\alpha=1}^{N} \frac{\partial^2}{\partial x_j^2} = N D_j^2 + \sum_{\alpha=1}^{N} D_{\alpha j}^2 . \tag{63}$$

When $d = 3$ we denote by $L_{\alpha 3}$ the projection of the angular momentum of the α particle on axis 3. Then, the projections of the total angular momentum and of the relative motion angular momentum on axis 3, are labeled as L_3 and L_3' respectively, determined as

$$\sum_{\alpha=1}^{N} L_{\alpha 3} = L_3 + L_3' , \;\; L_{\alpha 3} = x_{\alpha 1} p_{\alpha 2} - x_{\alpha 2} p_{\alpha 1} , \tag{64a}$$

$$L_3 = p_1 D_2 - p_2 D_1 , \; L_3' = \sum_{\alpha=1}^{N} \left(y_{\alpha 1} \xi_{\alpha 2} - y_{\alpha 2} \xi_{\alpha 1} \right) . \tag{64b}$$

The Hamilton function assigned to a many body system of N charged particles of mass M and equal electric charge Q, confined in a quadrupole combined (Paul and Penning) trap that displays axial (cylindrical) symmetry, in presence of a constant axial magnetic field B_0, can be expressed as [3,47]

$$H = \sum_{\alpha=1}^{N} \left[\frac{1}{2M} \sum_{j=1}^{3} p_{\alpha j}^2 + \frac{K_r}{2} \left(x_{\alpha 1}^2 + x_{\alpha 2}^2 \right) + \frac{K_a}{2} x_{\alpha 3}^2 - \frac{\omega_c}{2} L_{\alpha 3} \right] + W ,$$

with

$$K_r = \frac{M \omega_c^2}{4} - 2 Q c_2 A(t) , \; K_a = 4 Q c_2 A(t) , \; \omega_c = \frac{Q B_0}{M} ,$$

where ω_c is the cyclotron frequency characteristic to a Penning trap, c_2 is a constant that depends on the trap geometry and $A(t)$ represents a time periodical function [48]. We can also write H by adding the Hamilton function of the CM, H_{CM}, and the Hamilton function associated to the ion relative motion H':

$$H = H_{CM} + H' , \tag{65a}$$

Preprints (www.preprints.org) | NOT PEER-REVIEWED | Posted: 25 February 2021 doi:10.20944/preprints202102.0583.v1

$$H_{CM} = \frac{1}{2NM}\sum_{j=1}^{3} p_j^2 + \frac{NK_r}{2}\left(x_1^2 + x_2^2\right) + \frac{NK_a}{2}x_3^2 - \frac{\omega_c}{2}L_3\,, \tag{65b}$$

$$H' = \sum_{\alpha=1}^{N}\left[-\frac{\hbar^2}{2M}\sum_{j=1}^{3}\xi_{\alpha j}^2 + \frac{K_r}{2}\left(y_{\alpha 1}^2 + y_{\alpha 2}^2\right) + \frac{K_a}{2}y_{\alpha 3}^2\right] - \frac{\omega_c}{2}L_3' + W\,. \tag{65c}$$

Our results are in agreement with Ref. [35], where collective dynamical systems associated to the symplectic group are used to describe the axial and radial quantum Hamiltonians of the CM and of the relative ion motion. The space charge and its effect on the ion dynamics in case of a LIT is examined in Ref. [56], where the authors emphasize two distinguishable effects: (i) alteration of the specific ion oscillation frequency owing to variations of the trap potential, and (ii) for specific high charge density experimental conditions, the ions might perform as a single collective ensemble and exhibit dynamic frequency which is autonomous with respect to the number of ions. The model we suggest in this paper is appropriate to achieve a unitary approach aimed at generalizing the parameters for different types of 3D QIT. Further on, we apply this model to investigate the particular case of a combined Paul and Penning 3D QIT [57].

We consider W to be an interaction potential that is translation invariant (it only depends of $y_{\alpha j}$). The ion distribution in the trap can be represented by means of numerical analysis and computer modeling [58,59], through the Hamilton function we provide

$$H_{sim} = \sum_{i=1}^{n}\frac{1}{2M}{p_i}^2 + \sum_{i=1}^{n}\frac{M}{2}\left(\omega_1^2 x_i^2 + \omega_2^2 y_i^2 + \omega_3^2 z_i^2\right) + \sum_{1\le i<j\le n}\frac{Q^2}{4\pi\varepsilon_0}\frac{1}{\left|\vec{r}_i - \vec{r}_j\right|}\,, \tag{66}$$

where the second term accounts for the effective electric potential of the 3D QIT and the third term is responsible for the Coulomb repulsive force. In addition, we emphasize that the results obtained bring new contributions towards a better understanding of dynamical stability for charged particles levitated in a combined ion trap (Paul and Penning) [1], using both electrostatic DC and RF fields over which a constant static magnetic field is superimposed. Applications span areas of large interest such as stable confinement of antimatter and fundamental physics with antihydrogen [1,60]. We can also mention precision measurements and tests of the Standard Model using 3D QITs.

Many body systems consisting of N ions stored in a 3D QIT trap can be investigated locally in the neighbourhood of minimum configurations that characterize regular structures (Coulomb or ion crystals [18]). Collective models that exhibit a small number of degrees of freedom can be introduced to achieve a comprehensive portrait of the system, or the electric potential can be estimated by means of particular potentials for which the N-particle potentials are integrable. Little perturbations generally preserve quantum stability. The many body system under investigation is also characterized by a continuous part of the energy spectrum, whose classical equivalent is achieved through a class of chaotic orbits. Nevertheless, a weak correspondence can be traced between classical and quantum nonlinear dynamics, based on Husimi functions [3,35]. As a result, it comes straighforward to describe quantum ion crystals [61] by way of the minimum points associated to the Husimi function [48].

6. Results

6.1. Dynamical stability in the classical case

- We firstly discuss classical stability for two coupled oscillators confined in a 3D RF trap, using the dynamical systems theory. A familiar model is employed to portray system dynamics, that relies on a couple of control parameters: the axial angular

Preprints (www.preprints.org) | NOT PEER-REVIEWED | Posted: 25 February 2021 doi:10.20944/preprints202102.0583.v1

moment and the ratio between the radial and axial secular frequencies characteristic to the trap.

- We search for a stable solution of the equations of motion, and demonstrate it represents a superposition of two oscillations with secular frequencies ω_1 and ω_2, namely the system eigenfrequencies. We identify the modes of oscillation in case of strong coupling. For collective modes of motion the model estimates that only a peak of the mass is distinguishable, correlated with the average ion mass. In the weak coupling scenario each mode of the ion dynamics matches a single mass, which results in a shift of the resonance.
- Within the limit $m_1 = m_2$ we demonstrate the strong coupling requirement is always fulfilled regardless of the Coulomb coupling, which renders the weak coupling condition unsuitable in practice.
- For the stable solution chosen we illustrate phase portraits for the two ion system. When the eigenfrequencies ratio is a rational number ion dynamics is regular, characterized by periodic trajectories. If the ratio between the eigenfrequencies is an irrational number, then ion dynamics is *ergodic* as it exhibits iterative rotations around a specific point [50].
- We generally find ion dynamics to be quasiperiodic. By extending the motion in 3D we can ascertain that the trajectory executes quasiperiodic motion on the surface of a torus, referred to as a Kolmogorov-Arnold-Moser (KAM) torus. By choosing various initial conditions different KAM tori can be generated.
- We have integrated the equations of motion to explore ion dynamics and illustrate the associated power spectra. The numerical simulations performed demonstrate that ion dynamics is dominantly quasiperiodic.

6.2. Hamilton function. Hessian matrix of the potential

- The model previously applied is extended by using the Hessian matrix of the potential function to characterize the critical points of the system and implicitly the stability. For adimensional trap parameyter values $a, q \ll 1$, the equations of motion can be investigated in the pseudopotential approximation. Then, an autonomous Hamiltonian function results.
- Ihe Morse theory is used to determine the critical points of the U potential and discuss extensively the solutions of the equations of motion to fully characterize the two ion system dynamical stability.
- We show the degenerate critical points compose the bifurcation set whose image in the control parameter space establishes the catastrophe set of equations which defines the separatrix and we illustrate the bifurcation diagram for the system.

6.3. Semiclassical stability for a many body ion system

- We use the Hessian matrix approach that we previously introduced to investigate semiclassical stability and ordered structures for strongly coupled Coulomb systems(SCCS) confined in 3D QIT and suggest an analytical a method to determine the associated critical points.
- We find the elements of the Hessian matrix of the potential function U in a critical point

6.4. Collective dynamics for systems of ions confined in a 3D QIT

- We apply our model to explore dynamical stability for systems consisting of N identical ions confined in a 3D QIT (Paul, Penning, or combined traps) and show they can be studied locally in the neighbourhood of the minimum configurations that describe ordered structures (Coulomb or ion crystals [18]). In order to perform a global description, we introduce collective models with a small number of degrees of freedom or the Coulomb potential can be approximated with specific potentials for which the N-particle potentials are integrable. Small enough perturbations

 doi:10.20944/preprints202102.0583.v1

maintain the quantum stability although the classical system may also exhibit a chaotic behaviour.

- We find the Hamilton function for a combined trap, which is the sum between the Hamilton function of the CM and the one corresponding to the relative motion of the ions. The ion distribution in the trap can be modeled by means of numerical analysis through the Hamilton function we provide
- The results obtained bring new contributions towards a better understanding of the dynamical stability of charged particles in 3D QIT, and in particular in combined ion traps, with applications such as stable trapping of antimatter. Our approach is very relevant in generalizing the parameters of different types of traps in a unified manner.

7. Discussion

We discuss dynamical stability for a classical system of two coupled oscillators in a 3D RF (Paul) trap using a well known model from literature [29–31], based on two control parameters: the axial angular moment and the ratio between the radial and axial secular frequencies of the trap. We enlarge the model by performing a qualitative analysis, based on the eigenvalues associated to the Hessian matrix of the potential, in order to explicitly determine the critical points, the minima and saddle points. The bifurcation set consists of the degenerate critical points. Its image in the control parameter space establishes the catastrophe set of equations which establishes the separatrix. We also supply the bifurcation diagram particularized to the system under investigation.

By illustrating the phase portraits we demonstrate that ion dynamics mainly consists of periodic trajectories, in the situation when the eigenfrequencies ratio is a rational number. In the scenario in which the eigenfrequencies ratio is an irrational number, the system is *ergodic* and it exhibits repetitive (iterative) rotations in the vicinity of a certain point. Our results also stand for ions with different masses or for electrical charges that are not identical, by generalizing the system investigated. By illustrating the phase portraits and the associated power spectra we show that ion dynamics is quasiperiodic for the parameter values employed in the numerical simulation.

The model we introduce is then used to investigate quantum stability for N identical ions levitated in a 3D QIT and we infer the elements of the Hessian matrix of the potential function U in a critical point. We then apply our model to explore dynamical stability for SCCS consisting of N identical ions confined in different types of 3D QIT (Paul, Penning, or combined traps) that exhibit cylindrical symmetry. We obtain the Hamilton function associated to a combined 3D QIT, which we show to be the sum of the Hamilton functions of the CM and of the relative motion of the ions. The ion distribution in the trap can be modeled by means of numerical analysis through the Hamilton function we provide. The paper suggests an alternative approach that is effective in describing the dynamical regimes for different types of traps in a coherent manner. The results obtained bring new contributions towards a better understanding of the dynamical stability (electrodynamics) of charged particles in a combinational ion trap (Paul and Penning). Applications span areas of vivid interest such as stable confinement of antimatter and fundamental physics with antihydrogen [1,60] or precision measurements and tests of the Standard Model. Better characterization of ion dynamics in such traps would lead to longer trapping times, which is an issue of outmost importance. Other possible applications are Coulomb or ion crystals (multi body dynamics). The results and methods used are relevant for the ion trap physics community to compare regimes without having the details of the trap itself.

We emphasize that the results obtained bring new contributions towards a better understanding of the dynamical stability of charged particles in a combined ion trap (Paul and Penning), using both electrostatic DC and RF fields over which a constant static magnetic field is superimposed. One of the advantages of our model lies in better characterizing ion dynamics for coupled two ion systems and for many body systems

 doi:10.20944/preprints202102.0583.v1

consisting of large number of ions. It also enables identifying stable solutions of motion and discussing the important issue of the critical points of the system.

Author Contributions: Conceptualization, B.M.; methodology, B.M. and S.L.; software, S.L.; validation, B.M. and S.L.; formal analysis, B.M.; investigation, B.M. and S.L.; resources, B.M. and S.L.; writing—original draft preparation, B.M.; writing—review and editing, B.M. and S.L.; visualization, S.L. and B.M.; project administration, B.M.; All authors have read and agreed to the published version of the manuscript.

Funding: This research was funded by the Romanian Space Agency (ROSA) contract number 136/2017 and by Ministerul Cercetării şi Inovării- contract number 16N/2019.

Conflicts of Interest: The authors declare no conflict of interest.

Abbreviations

The following abbreviations are used in this manuscript:

3D	3 Dimensional
CM	Centre of Mass
LIT	Linear Ion Trap
QIP	Quantum Information Processing
QIT	Quadrupole Ion Trap
RF	Radiofrequency
SCCS	Strongly Coupled Coulomb Systems
SET	Surface Electrode Trap

Appendix A. Dynamical stability

As shown in Sec. 2.1, the expression of the autonomous Hamiltonian function associated to the system of two ions is given by eq. 24, where $r = \sqrt{\rho^2 + z^2}$, $\lambda = \mu_z/\mu_x$, $\mu_z = \sqrt{2(q^2 - a)}$. In fact λ and ν represet the two control parameters chosen, with λ the ratio between the secular axial and radial frequencies of the trap. ν denotes the scaled axial (z) component of the angular momentum L_z, while μ_z represents the second (or axial) secular frequency [29]. By calculus we infer

$$\lambda^2 = 4\frac{q^2 - a}{q^2 + 2a}, \quad \nu^2 = \frac{2L_z^2}{q^2 + 2a}\,, \tag{A1}$$

and we discriminate among three cases [30]:

1. $\lambda = \frac{1}{2}$ and from eq. (A1) we infer
$$a = \frac{5q^2}{6}$$
2. $\lambda = 1$. Eq.(A1) gives
$$a = \frac{q^2}{2}$$
3. $\lambda = 2$. By an analogous procedure we have
$$a = 0\,.$$

Appendix B. Quantum Stability

Using eqs. 44 and 45 we obtain

$$\frac{\partial}{\partial q_{\gamma j}}\frac{1}{|\vec{r}_\alpha - \vec{r}_\beta|} = -\frac{1}{|\vec{r}_\alpha - \vec{r}_\beta|^2}\frac{\partial}{\partial q_{\gamma j}}|\vec{r}_\alpha - \vec{r}_\beta| \tag{A2}$$

Preprints (www.preprints.org) | NOT PEER-REVIEWED | Posted: 25 February 2021 doi:10.20944/preprints202102.0583.v1

We also have

$$|\vec{r}_\alpha - \vec{r}_\beta| = \sqrt{\sum_{h=1}^{3} \left(q_{\alpha h} - q_{\beta h}\right)^2} \,. \tag{A3}$$

Then

$$\frac{\partial}{\partial q_{\gamma j}} |\vec{r}_\alpha - \vec{r}_\beta| = |\vec{r}_\alpha - \vec{r}_\beta|^{-1} \left(q_{\alpha j} - q_{\beta j}\right) \left(\delta_{\alpha\gamma} - \delta_{\beta\gamma}\right) , \tag{A4}$$

and

$$\frac{\partial}{\partial q_{\gamma j}} \frac{1}{|\vec{r}_\alpha - \vec{r}_\beta|} = -\frac{1}{|\vec{r}_\alpha - \vec{r}_\beta|^3} \left(q_{\alpha j} - q_{\beta j}\right) \left(\delta_{\alpha\gamma} - \delta_{\beta\gamma}\right) . \tag{A5}$$

By using eq. (47) the last term in eq. (51) can be expressed as

$$\frac{\partial \xi_{\alpha\gamma}}{\partial q_{\gamma' j'}} = \frac{Q_\alpha Q_\gamma}{4\pi\varepsilon_0} \frac{\partial}{\partial q_{\gamma' j'}} \frac{1}{|\vec{r}_\alpha - \vec{r}_\gamma|^3} \,. \tag{A6}$$

Moreover

$$\frac{\partial}{\partial q_{\gamma' j'}} |\vec{r}_\alpha - \vec{r}_\gamma|^{-3} = -3|\vec{r}_\alpha - \vec{r}_\gamma|^{-5} \left(q_{\alpha j'} - q_{\gamma j'}\right) \left(\delta_{\alpha\gamma'} - \delta_{\gamma\gamma'}\right) . \tag{A7}$$

Then, eq. (A6) can be cast into

$$\frac{\partial \xi_{\alpha\gamma}}{\partial q_{\gamma' j'}} = -\eta_{\alpha\gamma} \left(q_{\alpha j'} - q_{\gamma j'}\right) \left(\delta_{\alpha\gamma'} - \delta_{\gamma\gamma'}\right); \; \eta_{\alpha\gamma} = \frac{Q_\alpha Q_\gamma}{4\pi\varepsilon_0} \, 3|\vec{r}_\alpha - \vec{r}_\gamma|^{-5}, \; \alpha \neq \gamma \,. \tag{A8}$$

We use

$$\sum_{\alpha=1}^{N} q_\alpha \delta_{\alpha\gamma} = q_\gamma \,, \tag{A9}$$

References

1. Quint, W.; Vogel, M., Eds. *Fundamental Physics in Particle Traps*; Vol. 256, *Springer Tracts in Modern Physics*, Springer: Berlin Heidelberg, 2014. doi:10.1007/978-3-642-45201-7.
2. Kozlov, M.G.; Safronova, M.S.; Crespo López-Urrutia, J.R.; Schmidt, P.O. Highly charged ions: Optical clocks and applications in fundamental physics. *Rev. Mod. Phys.* **2018**, *90*, 045005. doi:10.1103/RevModPhys.90.045005.
3. Major, F.G.; Gheorghe, V.N.; Werth, G. *Charged Particle Traps: Physics and Techniques of Charged Particle Field Confinement*; Vol. 37, *Springer Series on Atomic, Optical and Plasma Physics*, Springer: Berlin Heidelberg, 2005. doi:10.1007/b137836.
4. Orszag, M. *Quantum Optics: Including Noise Reduction, Trapped Ions, Quantum Trajectories, and Decoherence*, 3rd ed.; Springer Intl. Publishing: Berlin Heidelberg, 2016. doi:10.1007/978-3-319-29037-9.
5. Safronova, M.S.; Budker, D.; DeMille, D.; Kimball, D.F.J.; Derevianko, A.; Clark, C.W. Search for new physics with atoms and molecules. *Rev. Mod. Phys.* **2018**, *90*, 025008. doi:10.1103/RevModPhys.90.025008.
6. Wineland, D.J.; Leibfried, D. Quantum information processing and metrology with trapped ions. *Laser Phys. Lett.* **2011**, *8*, 175 – 188. doi:10.1002/lapl.201010125.
7. Sinclair, A. An Introduction to Trapped Ions, Scalability and Quantum Metrology. Quantum Information and Coherence; Andersson, E.; Öhberg, P., Eds. Springer, 2011, Vol. 67, *Scottish Graduate Series*, pp. 211 – 246. doi:10.1007/978-3-319-04063-9_9.
8. Mehlstäubler, T.E.; Grosche, G.; Lisdat, C.; Schmidt, P.O.; Denker, H. Highly charged ions: Optical clocks and applications in fundamental physics. *Rep. Prog. Phys.* **2018**, *81*, 064401. doi:10.1088/1361-6633/aab409.
9. Nam, Y.S.; Weiss, D.K.; Blümel, R. Explicit, analytical radio-frequency heating formulas for spherically symmetric nonneutral plasmas in a Paul trap. *Phys. Lett. A* **2017**, *381*, 3477 – 3481. doi:10.1016/j.physleta.2017.09.001.
10. Mihalcea, B.; Filinov, V.; Syrovatka, R.; Vasilyak, L. The physics and applications of strongly coupled plasmas levitated in electrodynamic traps, [1910.14320].
11. Haroche, S.; Raimond, J.M. *Exploring the Quantum: Atoms, Cavities and Photons*; Oxford Graduate Texts, Oxford Univ. Press: Clarendon, Oxford, 2010. doi:10.1093/acprof:oso/9780198509141.001.0001.
12. Wineland, D.J. Nobel Lecture: Superposition, entanglement, and raising Schrödinger's cat. *Rev. Mod. Phys.* **2013**, *85*, 1103 – 1114. doi:10.1103/RevModPhys.85.1103.

13. Brown, K.R.; Kim, J.; Monroe, C. Co-designing a scalable quantum computer with trapped atomic ions. *npj Quantum Inf.* **2016**, *2*, 16034. doi:10.1038/npjqi.2016.34.
14. Bruzewicz, C.D.; Chiaverini, J.; McConnell, R.; Sage, J.M. Trapped-ion quantum computing: Progress and challenges. *Appl. Phys. Rev.* **2019**, *6*, 021314. doi:10.1063/1.5088164.
15. Warring, U.; Hakelberg, F.; Kiefer, P.; Wittemer, M.; Schaetz, T. Trapped Ion Architecture for Multi-Dimensional Quantum Simulations. *Adv. Quantum Technol.* **2020**, *3*, 1900137. doi:10.1002/qute.201900137.
16. Wan, Y.; Jördens, R.; Erickson, S.D.; Wu, J.J.; Bowler, R.; Tan, T.R.; Hou, P.Y.; Wineland, D.J.; Wilson, A.C.; Leibfried, D. Ion Transport and Reordering in a 2D Trap Array. *Adv. Quantum Technol.* **2020**, *3*, 2000028. doi:10.1002/qute.202000028.
17. Maitra, A.; Leibfried, D.; Ullmo, D.; Landa, H. Far-from-equilibrium noise-heating and laser-cooling dynamics in radio-frequency Paul traps. *Phys. Rev. A* **2019**, *99*, 043421. doi:10.1103/PhysRevA.99.043421.
18. Keller, J.; Burgermeister, T.; Kalincev, D.; Didier, A.; Kulosa, A.P.; Nordmann, T.; Kiethe, J.; Mehlstäubler, T.E. Controlling systematic frequency uncertainties at the 10^{-19} level in linear Coulomb crystals. *Phys. Rev. A* **2019**, *99*, 013405. doi:10.1103/PhysRevA.99.013405.
19. Schneider, C.; Porras, D.; Schaetz, T. Experimental quantum simulations of many-body physics with trapped ions. *Rep. Prog. Phys.* **2012**, *75*, 024401. doi:10.1088/0034-4885/75/2/024401.
20. Stoican, O.; Mihalcea, B.M.; Gheorghe, V. Miniaturized trapping setup with variable frequency. *Rom. Rep. Phys.* **2001**, *53*, 275 – 280.
21. Berman, G.P.; James, D.F.V.; Hughes, R.J.; Gulley, M.S.; Holzscheiter, M.H.; López, G.V. Dynamical stability and quantum chaos of ions in a linear trap. *Phys. Rev. A* **2000**, *61*, 023403. doi:10.1103/PhysRevA.61.023403.
22. Graß, T.; Juliá-Díaz, B.; Kuś, M.; Lewenstein, M. Quantum Chaos in SU(3) Models with Trapped Ions. *Phys. Rev. Lett.* **2013**, *111*, 090404. doi:10.1103/PhysRevLett.111.090404.
23. Santos, L.F.; Torres-Herrera, E.J. Nonequilibrium Quantum Dynamics of Many-Body Systems. In *Chaotic, Fractional, and Complex Dynamics: New Insights and Perspectives*; Edelman, M.; Macau, E.E.N.; Sanjuan, M.A.F., Eds.; Understanding Complex Systems, Springer Intl. Publishing: Cham, 2018; pp. 231–260. doi:10.1007/978-3-319-68109-2_12.
24. Conangla, G.P.; Nwaigwe, D.; Wehr, J.; Rica, R.A. Overdamped dynamics of a Brownian particle levitated in a Paul trap. *Phys. Rev. A* **2020**, *101*, 053823. doi:10.1103/PhysRevA.101.053823.
25. Gardiner, S.A.; Cirac, J.I.; Zoller, P. Quantum Chaos in an Ion Trap: The Delta-Kicked Harmonic Oscillator. *Phys. Rev. Lett.* **1997**, *79*, 4790 – 4793. doi:10.1103/PhysRevLett.79.4790.
26. Dodonov, V.V.; Man'ko, V.I.; Rosa, L. Quantum singular oscillator as a model of a two-ion trap: An amplification of transition probabilities due to small-time variations of the binding potential. *Phys. Rev. A* **1998**, *57*, 2851–2858. doi:10.1103/PhysRevA.57.2851.
27. Mihalcea, B.M. A quantum parametric oscillator in a radiofrequency trap. *Phys. Scr.* **2009**, *T135*, 014006. doi:10.1088/0031-8949/2009/T135/014006.
28. Mihalcea, B.M. Nonlinear harmonic boson oscillator. *Phys. Scr.* **2010**, *T140*, 014056. doi:10.1088/0031-8949/2010/T140/014056.
29. Blümel, R.; Kappler, C.; Quint, W.; Walther, H. Chaos and order of laser-cooled ions in a Paul trap. *Phys. Rev. A* **1989**, *40*, 808 – 823. doi:10.1103/PhysRevA.40.808.
30. Moore, M.; Blümel, R. Quantum manifestations of order and chaos in the Paul trap. *Phys. Rev. A* **1993**, *48*, 3082 – 3091. doi:10.1103/PhysRevA.48.3082.
31. Farrelly, D.; Howard, J.E. Double-well dynamics of two ions in the Paul and Penning traps. *Phys. Rev. A* **1994**, *49*, 1494 – 1497. doi:10.1103/PhysRevA.49.1494.
32. Blümel, R.; Bonneville, E.; Carmichael, A. Chaos and bifurcations in ion traps of cylindrical and spherical design. *Phys. Rev. E* **1998**, *57*, 1511 – 1518. doi:10.1103/PhysRevE.57.1511.
33. Walz, J.; Siemers, I.; Schubert, M.; Neuhauser, W.; Blatt, R.; Teloy, E. Ion storage in the rf octupole trap. *Phys. Rev. A* **1994**, *50*, 4122 – 4132. doi:10.1103/PhysRevA.50.4122.
34. Mihalcea, B.M.; Niculae, C.M.; Gheorghe, V.N. On the Multipolar Electromagnetic Traps. *Rom. Journ. Phys.* **1999**, *44*, 543 – 550.
35. Gheorghe, V.N.; Werth, G. Quasienergy states of trapped ions. *Eur. Phys. J. D* **2000**, *10*, 197 – 203. doi:10.1007/s100530050541.
36. Menicucci, N.C.; Milburn, G.J. Single trapped ion as a time-dependent harmonic oscillator. *Phys. Rev. A* **2007**, *76*, 052105. doi:10.1103/PhysRevA.76.052105.
37. Mihalcea, B.M.; Vişan, G.G. Nonlinear ion trap stability analysis. *Phys. Scr.* **2010**, *T140*, 014057. doi:10.1088/0031-8949/2010/T140/014057.
38. Akerman, N.; Kotler, S.; Glickman, Y.; Dallal, Y.; Keselman, A.; Ozeri, R. Single-ion nonlinear mechanical oscillator. *Phys. Rev. A* **2010**, *82*, 061402(R). doi:10.1103/PhysRevA.82.061402.
39. Ishizaki, R.; Sata, H.; Shoji, T. Chaos-Induced Diffusion in a Nonlinear Dissipative Mathieu Equation for a Charged Fine Particle in an AC Trap. *J. Phys. Soc. Jpn.* **2011**, *80*, 044001. doi:10.1143/JPSJ.80.044001.
40. Shaikh, F.A.; Ozakin, A. Stability analysis of ion motion in asymmetric planar ion traps. *J. Appl. Phys.* **2012**, *112*, 074904. doi:10.1063/1.4752404.
41. Landa, H.; Drewsen, M.; Reznik, B.; Retzker, A. Modes of oscillation in radiofrequency Paul traps. *New J. Phys.* **2012**, *14*, 093023. doi:10.1088/1367-2630/14/9/093023.
42. Roberdel, V.; Leibfried, D.; Ullmo, D.; Landa, H. Phase space study of surface electrode Paul traps: Integrable, chaotic, and mixed motion. *Phys. Rev. A* **2018**, *97*, 053419. doi:10.1103/PhysRevA.97.053419.

43. Rozhdestvenskii, Y.V.; Rudyi, S.S. Nonlinear Ion Dynamics in a Radiofrequency Multipole Trap. *Tech. Phys. Lett.* **2017**, *43*, 748 – 752. doi:10.1134/S1063785017080259.
44. Fountas, P.N.; Poggio, M.; Willitsch, S. Classical and quantum dynamics of a trapped ion coupled to a charged nanowire. *New J. Phys.* **2019**, *21*, 013030. doi:10.1088/1367-2630/aaf8f5.
45. Zelaya, K.; Rosas-Ortiz, O. Quantum nonstationary oscillators: Invariants, dynamical algebras and coherent states via point transformations. *Phys. Scr.* **2020**, *95*, 064004. doi:10.1088/1402-4896/ab5cbf.
46. Gheorghe, V.N.; Vedel, F. Quantum dynamics of trapped ions. *Phys. Rev. A* **1992**, *45*, 4828 – 4831. doi:10.1103/PhysRevA.45.4828.
47. Mihalcea, B.M. Semiclassical dynamics for an ion confined within a nonlinear electromagnetic trap. *Phys. Scr.* **2011**, *T143*, 014018. doi:10.1088/0031-8949/2011/T143/014018.
48. Mihalcea, B.M. Squeezed coherent states of motion for ions confined in quadrupole and octupole ion traps. *Ann. Phys.* **2018**, *388*, 100 – 113. doi:10.1016/j.aop.2017.11.004.
49. Landa, H.; Drewsen, M.; Reznik, B.; Retzker, A. Classical and quantum modes of coupled Mathieu equations. *J. Phys. A: Math. Theor.* **2012**, *45*, 455305. doi:10.1088/1751-8113/45/45/455305.
50. Gutzwiller, M.C. In *Chaos in Classical and Quantum Mechanics*; John, F.; Kadanoff, L.; Marsden, J.E.; Sirovich, L.; Wiggins, S., Eds.; Springer-Verlag: New York, 1990; Vol. 1, *Interdisciplinary Applied Mathematics*. doi:10.1007/978-1-4612-0983-6.
51. Dumas, S.H. *The KAM Story: A Friendly Introduction to the Content, History, and Significance of Classical Kolmogorov-Arnold-Moser Theory*; World Scientific: Singapore, 2014. doi:10.1142/8955.
52. Lynch, S. *Dynamical Systems with Applications using MATLAB*, 2nd ed.; Birkhäuser - Springer: Cham, 2014. doi:10.1007/978-3-319-06820-6.
53. Foot, C.J.; Trypogeorgos, D.; Bentine, E.; Gardner, A.; Keller, M. Two-frequency operation of a Paul trap to optimise confinement of two species of ions. *Int. J. Mass. Spectr.* **2018**, *430*, 117 – 125. doi:10.1016/j.ijms.2018.05.007.
54. Blümel, R. Loading a Paul Trap: Densities, Capacities, and Scaling in the Saturation Regime. *Atoms* **2021**, *9*, 11.
55. Chang, K.C. *Infinite Dimensional Morse Theory and Multiple Solution Problems*; Vol. 6, *Progress in Nonlinear Differential Equations and Their Applications*, Birkhäuser: Boston, MA, 1993. doi:10.1007/978-1-4612-0385-8.
56. Mandal, P.; Das, S.; De Munshi, D.; Dutta, T.; Mukherjee, M. Space charge and collective oscillation of ion cloud in a linear Paul trap. *Int. J. Mass Spectrom.* **2014**, *364*, 16 – 20. doi:10.1016/j.ijms.2014.03.010.
57. Li, G.Z.; Guan, S.; Marshall, A.G. Comparison of Equilibrium Ion Density Distribution and Trapping Force in Penning, Paul, and Combined Ion Traps. *J. Am. Soc. Mass Spectrom.* **1998**, *9*, 473 – 481. doi:10.1016/S1044-0305(98)00005-1.
58. Singer, K.; Poschinger, U.; Murphy, M.; Ivanov, P.; Ziesel, F.; Calarco, T.; Schmidt-Kaler, F. *Colloquium*: Trapped ions as quantum bits: Essential numerical tools. *Rev. Mod. Phys.* **2010**, *82*, 2609 – 2632. doi:10.1103/RevModPhys.82.2609.
59. Lynch, S. *Dynamical Systems with Applications using Python*; Birkhäuser: Basel, 2018. doi:10.1007/978-3-319-78145-7.
60. Saxena, V. Analytical Approximate Solution of a Coupled Two Frequency Hill's Equation, [2008.05525].
61. Yoshimura, B.; Stork, M.; Dadic, D.; Campbell, W.C.; Freericks, J.K. Creation of two-dimensional Coulomb crystals of ions in oblate Paul traps for quantum simulations. *EPJ Quantum Technology* **2015**, *2*, 2. doi:10.1140/epjqt14.